1902. Equivalent stiffness and dynamic response of new mechanical elastic wheel

Qiang Wang[1], Youqun Zhao[2], Xianbin Du[3], Mingmin Zhu[4], Hongxun Fu[5]
College of Energy and Power Engineering, Nanjing University of Aeronautics and Astronautics, Nanjing, 210016, China
[2]Corresponding author
E-mail: [1]*wq8121318@163.com*, [2]*yqzhao@nuaa.edu.cn*, [3]*duxianbin2010@126.com*, [4]*zhumingmin1986@163.com*, [5]*fuhongxun615@163.com*

(Received 28 July 2015; received in revised form 6 December 2015; accepted 14 December 2015)

Abstract. To investigate the stiffness characteristics of the new mechanical elastic wheel (MEW), the elastic foundation closed circle curved beam model of MEW was established by curved beam theory. With the Laplace transformation and boundary conditions of the governing differential equations, the analytical relations among the radial deformation, bending stiffness of elastic wheel, the elastic foundation stiffness of hinges, elastic wheel laminated structure parameters and excitation frequency were analyzed. The correctness of the curved beam model was validated by the finite element method. Curved beam model validation and the application of the nonlinear finite element model show that the influence of elastic wheel laminated structure and deformation on dynamic response is equal to the equivalent stiffness. The results indicate that the equivalent stiffness and dynamic response of MEW become increased nonlinearly with component content of elastic bead ring, moreover, the equivalent stiffness and dynamic response of MEW increase nonlinearly with the deformation amount of MEW, and the dynamic response significantly decreases with the increase of excitation frequency, under this circumstance that the laminated structure of elastic wheel has been unchanged.

Keywords: mechanical elastic wheel, elastic wheel laminated structure, curved beam model, equivalent stiffness, dynamic response.

1. Introduction

The tire is the main component of vibration reduction, and the dynamic characteristics of the tire affect not only the operating stability, but also the driving smoothness and riding comfortableness of vehicle to a certain extent. Nevertheless, the vehicle passing ability will reduce, even losing the mobility when the tire is punctured damaged. Then the spare tire will increase the load and fuel consumption of the vehicle. Furthermore, the vehicle still exists the blowout risk of tire at high speed. To change the situation of the existing tire, developing run-flat and anti-puncture tire to guarantee high performance and security has become a consensus of the world's major tire manufacturers. Therefore, researchers have recently focused their attention on non-pneumatic tires with different structures. But the non-pneumatic tires have the disadvantage of excessive weight, complex processing technology or cooling difficult and so on, moreover, the proceeding is still in the stage of research and development. To solve the above problems, a mechanical elastic wheel (MEW) for the off-road vehicle is proposed. The MEW can realize the basic function of traditional pneumatic tire, in additional, the problems such as stinging, puncturing and blasting damage have been avoided. Thus, the MEW is greatly satisfied with requirements of safe service for the special vehicles, such as military vehicles, off-road vehicles, emergency service and disaster relief vehicle.

Radial stiffness and damping coefficient are vital parameters to describe tire dynamic characteristics, and it has become a significant research topic on tire stiffness and its dynamic characteristics. There is a flood of theoretical and computational literature on the stiffness and dynamic characteristics of pneumatic tires [1-4]. Nonlinear analytic model for tire stiffness and damping was established, the model had built the numerical analytical relations among stiffness, deformation, excitation frequency and inflation pressure. The radial stiffness of tire was concerned

with its section width, rim diameter and service life; and the damping coefficient was mainly depended on the damping properties of the tire materials [5-7]. But researchers have rarely focused their attention on the nonlinear stiffness and damping characteristics of non-pneumatic tires. Doo-Man Kim et al. studied the static stiffness of the non-pneumatic tires using the theory of curved beam model and the simulation analysis method. The influence of honeycomb structure on the radial stiffness was analyzed [13-15]. Paul F. Joseph et al. deduced the calculation model of the radial displacement of the non-pneumatic tire by curved beam model, and the non-pneumatic tire radial stiffness was calculated, the influence of flexible ring material properties and the number of spokes on the radial stiffness were analyzed [16-17].

Systematic research on the mechanical properties, trafficability and traction ability of MEW, the results indicate that the proposed wheel has good trafficability, traction ability and small rolling resistance [10-12]. To further investigate the stiffness characteristics of the MEW, the elastic foundation closed circle curved beam model of MEW was established by curved beam theory in this paper. The numerical analytical relations among the radial deformation, bending stiffness of elastic wheel, the elastic foundation stiffness of hinge group, elastic wheel laminated structure parameters and excitation frequency were analyzed. In order to validate the results, the finite element model of the wheel considering material nonlinearity, geometric nonlinearity and contact nonlinearity is established, the present analytical solution is compared with that of the finite element analysis results. The effect of elastic wheel laminated structure on equivalent stiffness and dynamic response is presented.

2. Structure and loading analysis of mechanical elastic wheel

MEW is mainly consisted of elastic wheel (rubber tread, elastic bead ring, clasps), hub, pins, hinges and other accessories as shown in Fig. 1.

In the process of the operated MEW, according to the vertical load and torque that transfers from axle to hub, the state of hinges are changed from equilibrium to preload. It makes elastic wheel is pulled, and thus generating pulling force. These forces which are defined as tangential component along the cylindrical wheel overcome the static friction force of the wheel with the ground to impelling the wheel forward. Within the elastic wheel, the suspended hubs depend on tensile strength of hinges. When they are affected by the vertical load, the hub will slip a distance relative to the free condition downward. The hinges that closer to the ground are slightly curved, elastic deformation occurs in the upper part of elastic wheel by the downward tension of hub, it is similar to the elliptic type. When the wheel is rolling, the elastic wheel will endure most of the excitation from the ground, display elastic deformation instantaneously, and instantaneous bending of hinges has been relieved accordingly. Therefore, the performance of buffer damping of MEW is different from the ordinary pneumatic tire [10].

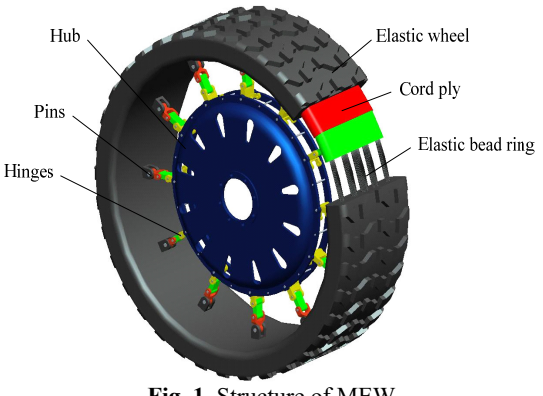

Fig. 1. Structure of MEW

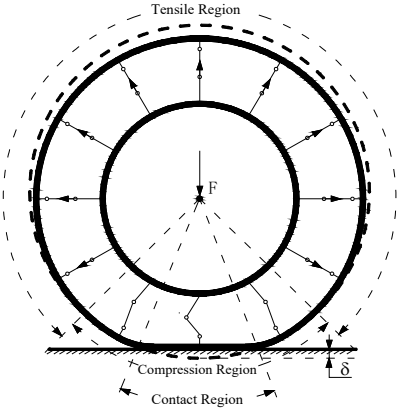

Fig. 2. Loading and deformation of MEW

The load transfer to elastic wheel through hinges under the static load conditions, the obvious flexure deformation appeared in the tangent parts between wheel and the ground due to the load. The deformed tendency of the radial shrink appeared in the upper parts that are relative to the free conditions. Based on the design of wheel structure, the hinges only load on pulling force rather than pressure. The hub suspends in elastic wheel under the function of load, at the top of elastic wheel, they endure the load. The carrying way has become not only high efficiency and excellent adhesion ability, but also favorable buffer damping and passing ability of wheel, as shown in Fig. 2. According to the force analysis of MEW, the equivalent stiffness consists of radial stiffness of elastic wheel and elastic basal stiffness of hinges, it is as known as static stiffness of wheel. It mainly depends on the component content of the laminated structure of elastic wheel and structure characteristics of hinges. The equivalent stiffness of wheel has become increased with equivalent modulus, the variable quantity between equivalent stiffness of MEW and stiffness of elastic wheel is approximately equal. The response of wheel is considered to be the dynamic response under a harmonic force, and the change regularity of dynamic stiffness is equal to the change state of dynamic response. In order to make the influence of laminated structure of elastic wheel on equivalent stiffness more certainty, based on the mechanism of the wheel, research on the influence of the component content of the laminated structure on equivalent stiffness and dynamic response of wheel, in the conditions that the number and structure characteristics of hinges make explicit.

3. Establishment of the mechanical elastic wheel model

It is assumed that contact region of the wheel with ground is a closed-form circular ring curved beam contact with rigid plane, and the contact region is continuous. Assuming the thickness of elastic wheel is far less than the radius of the wheel, in this study the effect of tread pattern is neglected and the hub is assumed to be rigid, and therefore, the elastic wheel is simplified to the Timoshenko curved beam model as shown in Fig. 3 [16].

In view of the bending deformation of circular curved beam, the circular beam is geometrically characterized by its uniform cross-section, area of the annular band A, constant width B and constant thickness h. R denotes the radius of curvature of the centroid of the cross-section. Where $\sigma_{\theta\theta}$, $\tau_{r\theta}$, N, M and V are respectively the normal stress, transverse shearing, the internal axial force, the internal moment at the centroid of the cross-sections of the ring and the internal transverse shearing force, in terms of the stress resultants for axial force, bending moment and shear force:

$$\begin{cases} N = \int_A \sigma_{\theta\theta} dA, \\ M = \int_A z\sigma_{\theta\theta} dA, \\ V = \int_A \tau_{r\theta} dA\,. \end{cases} \tag{1}$$

Making use of a cylindrical coordinate system, at an arbitrary angular location θ, where r, $u_r(\theta)$, $u_{\theta 0}(\theta)$ and $\phi(\theta)$ are respectively the cross-section curvature radius, transverse displacement, circumferential displacement and cross-section rotation with respect to the centroid of the cross-section, introducing the thickness variable $z = r - R$, the associated displacement field is given by:

$$\begin{cases} u_r(z,\theta) = u_r(\theta), \\ u_\theta(z,\theta) = u_{\theta 0}(\theta) + z\phi(\theta). \end{cases} \tag{2}$$

The following approximations for the strains:

$$\begin{cases}\varepsilon_{rr}=0,\\ \varepsilon_{\theta\theta}=\dfrac{1}{R+z}\left(\dfrac{du_{\theta 0}}{d\theta}+u_r+z\dfrac{d\phi}{d\theta}\right),\\ \gamma_{r\theta}=\dfrac{1}{R+z}\left(\dfrac{du_r}{d\theta}-u_{\theta 0}+R\phi\right).\end{cases} \tag{3}$$

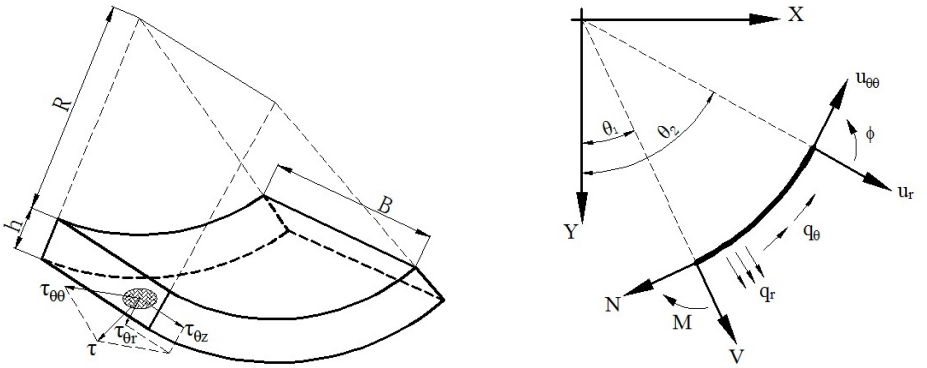

Fig. 3. Elastic wheel disk uniformly curved beam model

The stress distribution is given by:

$$\begin{cases}\sigma_{rr}=E\varepsilon_{rr}=0,\\ \sigma_{\theta\theta}=E\varepsilon_{\theta\theta}=\varepsilon_{\theta\theta}=\dfrac{E}{R+z}\left(\dfrac{du_{\theta 0}}{d\theta}+u_r+z\dfrac{d\phi}{d\theta}\right),\\ \tau_{r\theta}=G\gamma_{r\theta}=\dfrac{G}{R+z}\left(\dfrac{du_r}{d\theta}-u_{\theta 0}+R\phi\right).\end{cases} \tag{4}$$

Introducing the variable:

$$\int_A\frac{E}{R+z}dA=\frac{EA}{R},\quad \int_A\frac{z^2E}{R+z}dA=\frac{EI}{R},\quad \int_A\frac{zE}{R+z}dA=0,\quad \int_A\frac{G}{R+z}dA=\frac{GA}{R},$$

where I, EA, EI and GA are respectively the area moment of inertia of the cross sectional, the circumferential stiffness, the bending stiffness and the shear stiffness, the stress resultants consistent with Eq. (1) is given by:

$$\begin{cases}N=\displaystyle\int_A\sigma_{\theta\theta}dA=\int_A\frac{E}{R+z}\left(\frac{du_{\theta 0}}{d\theta}+u_r+z\frac{d\phi}{d\theta}\right)dA=\frac{EA}{R}\left(\frac{r}{R}\frac{du_{\theta 0}}{d\theta}+u_r\right),\\ M=\displaystyle\int_A z\sigma_{\theta\theta}dA=\int_A\frac{zE}{R+z}\left(\frac{du_{\theta 0}}{d\theta}+u_r+z\frac{d\phi}{d\theta}\right)dA=\frac{EI}{R^2}\frac{d^2u_r}{d\theta^2},\\ V=\displaystyle\int_A\tau_{r\theta}dA=\int_A\frac{G}{R+z}\left(\frac{du_r}{d\theta}-u_{\theta 0}+R\phi\right)dA=\frac{GA}{R}\left(\frac{du_r}{d\theta}-u_{\theta 0}+R\phi\right).\end{cases} \tag{5}$$

3.1. Non-contact region

The non-contact region of the wheel with ground develops as illustrated in Fig. 2, when bending deformation of circular curved beam can only bear radial force, and the circumferential force is neglected. Analysis of the right part of the wheel, in the non-contact region, $\varphi_T\le\theta\le\pi$, according to the force analysis of circular curved beam element, the static equilibrium equations are given by:

$$\begin{cases} \dfrac{dN(\theta)}{d\theta} + V(\theta) = 0, \\ \dfrac{dV(\theta)}{d\theta} = -ku_r + N(\theta), \\ \dfrac{dM(\theta)}{Rd\theta} = V(\theta). \end{cases} \tag{6}$$

Thus, the governing equations consistent with Eq. (6) are given by:

$$\begin{cases} EA\dfrac{d^2u_{\theta 0}}{d\theta^2} - GAu_{\theta 0} + (EA + GA)\dfrac{du_r}{d\theta} + RGA\phi = 0, \\ -GA\dfrac{d^2u_r}{d\theta^2} + EAu_r + (EA + GA)\dfrac{du_{\theta 0}}{d\theta} - RGA\dfrac{d\phi}{d\theta} = -R^2ku_r, \\ EI\dfrac{d^2\phi}{d\theta^2} - R^2GA\phi - RGA\dfrac{du_r}{d\theta} + RGAu_{\theta 0} = 0. \end{cases} \tag{7}$$

3.2. Contact region

Under the load effects, the circular curved beam produces obviously bending deformation, in the non-contact region, $0 \le \theta \le \varphi_T$, according to the force analysis of circular curved beam element, the static equilibrium equations are given by:

$$\begin{cases} \dfrac{dN(\theta)}{d\theta} + V(\theta) = -RBq_\theta, \\ \dfrac{dV(\theta)}{d\theta} = -RBq_r + N(\theta), \\ \dfrac{dM(\theta)}{Rd\theta} = V(\theta). \end{cases} \tag{8}$$

The governing equations consistent with Eq. (8) are given by:

$$\begin{cases} EA\dfrac{d^2u_{\theta 0}}{d\theta^2} - GAu_{\theta 0} + (EA + GA)\dfrac{du_r}{d\theta} + RGA\phi = -R^2Bq_\theta, \\ -GA\dfrac{d^2u_r}{d\theta^2} + EAu_r + (EA + GA)\dfrac{du_{\theta 0}}{d\theta} - RGA\dfrac{d\phi}{d\theta} = -R^2Bq_r, \\ EI\dfrac{d^2\phi}{d\theta^2} - R^2GA\phi - RGA\dfrac{du_r}{d\theta} + RGAu_{\theta 0} = 0. \end{cases} \tag{9}$$

The cross-section rotation ϕ with respect to the centroid of the cross-section after deformation is composed primarily of the rotation angle caused by the radial displacement increment du_r and the rotation angle caused by the axial displacement $u_{\theta 0}$:

$$\phi = -\frac{1}{R}\left(\frac{du_r}{d\theta} - u_{\theta 0}\right). \tag{10}$$

According to the actual static load of the wheel, these equations are subjected to the following boundary conditions:

$$\begin{cases} \left.\dfrac{du_{\theta 0}}{d\theta}\right|_{\theta=\varphi_C} = \left.\dfrac{du_{\theta 0}}{d\theta}\right|_{\theta=\pi} = 0, \\ u_r(\theta=\varphi_C) = u_r(\theta=\varphi_T), \\ V(\varphi_C) = V(\varphi_T) = 0, \quad V(0) = -\dfrac{q_r}{2}x(t), \\ N(\varphi_C) = N(\varphi_T), \\ M(\varphi_C) = M(\varphi_T), \\ \int_0^{\pi} u_{\theta 0}(\theta)d\theta = 0\,. \end{cases} \tag{11}$$

The uncoupled equation for the transverse displacement can be expressed as follows:

$$\frac{d^5u_r(\theta)}{d\theta^5} + 2\frac{d^3u_r(\theta)}{d\theta^3} + (1+\lambda^2)\frac{du_r(\theta)}{d\theta} \approx 0, \tag{12}$$

where $\lambda^2 = kR^3/EI$ reflects the ratio of the elastic foundation stiffness of hinges with the bending stiffness of elastic wheel.

While the hypothetical solution for Eq. (12) can be expressed as $u_r(\theta) = e^{\kappa\theta}$, the following notation is used to represent the general solution assuming Eq. (12):

$$\alpha = \sqrt{\frac{\left(\sqrt{1+\lambda^2}-1\right)}{2}}, \quad \beta = \sqrt{\frac{\left(\sqrt{1+\lambda^2}+1\right)}{2}}. \tag{13}$$

Introducing the unknown coefficients c_1-c_5, the general solution can be expressed as follows:

$$u_r(\theta) = c_1 + c_2e^{(\alpha+i\beta)\theta} + c_3e^{(\alpha-i\beta)\theta} + c_4e^{-(\alpha+i\beta)\theta} + c_5e^{-(\alpha-i\beta)\theta}, \tag{14}$$

where the following solution is given by:

$$u_r(\theta) = \frac{F_s\lambda^2}{8\alpha\beta k(\alpha^2+\beta^2)}\left[-\frac{4\alpha\beta}{(\alpha^2+\beta^2)\pi} + \frac{(\alpha i+\beta)e^{-(\alpha+i\beta)\pi}}{e^{(\alpha+i\beta)\pi}-e^{-(\alpha+i\beta)\pi}}\right.$$
$$\left. -\frac{(\alpha i-\beta)e^{-(\alpha-i\beta)\pi}e^{(\alpha-i\beta)\theta}}{e^{(\alpha-i\beta)\pi}-e^{-(\alpha-i\beta)\pi}} + \frac{(\alpha i+\beta)e^{(\alpha+i\beta)\pi}e^{-(\alpha+i\beta)\theta}}{e^{(\alpha+i\beta)\pi}-e^{-(\alpha+i\beta)\pi}} - \frac{(\alpha i-\beta)e^{(\alpha-i\beta)\pi}e^{-(\alpha-i\beta)\theta}}{e^{(\alpha-i\beta)\pi}-e^{-(\alpha-i\beta)\pi}}\right], \tag{15}$$

If $F_s = 1$ in the Eq. (15), the radial displacement ($\theta = 0$) is equal to the equivalent flexibility of wheel, which gives the following solution:

$$C = \frac{\lambda^2}{8\alpha\beta k(\alpha^2+\beta^2)}\left[-\frac{4\alpha\beta}{(\alpha^2+\beta^2)\pi} + \frac{(\alpha i+\beta)e^{-(\alpha+i\beta)\pi}}{e^{(\alpha+i\beta)\pi}-e^{-(\alpha+i\beta)\pi}}\right.$$
$$\left. -\frac{(\alpha i-\beta)e^{-(\alpha-i\beta)\pi}}{e^{(\alpha-i\beta)\pi}-e^{-(\alpha-i\beta)\pi}} + \frac{(\alpha i+\beta)e^{(\alpha+i\beta)\pi}}{e^{(\alpha+i\beta)\pi}-e^{-(\alpha+i\beta)\pi}} - \frac{(\alpha i-\beta)e^{(\alpha-i\beta)\pi}}{e^{(\alpha-i\beta)\pi}-e^{-(\alpha-i\beta)\pi}}\right]. \tag{16}$$

The reciprocal of equivalent flexibility can be regarded as the equivalent stiffness of the wheel, under the load effects, the circular curved beam produces the vertical downward translation and bending deformation. The bending deformation of curved beam decreases with the decrease of the stiffness ratio λ, and the analysis results show the size of the stiffness ratio λ has greater influence on the sink of MEW.

3.3. Dynamic response modeling

In view of the Dynamic response of circular curved beam, the hub is fixed, applying the harmonic impact load ($F_d = q'_r x(t)$) to the elastic wheel, $x(t)$ is the sine function. The inertia ($-\rho_l(d^2u_r/dt^2)$) of unit arc length needs to be considered when the force acting on the elastic curved beam model, where ρ_l and d^2u_r/dt^2 are respectively the linear density of the elastic wheel and the acceleration caused by the radial displacement. Where t and θ are respectively time and space coordinates, the static equilibrium equations are given by:

$$\begin{cases} \dfrac{dN(\theta,t)}{d\theta} = -V(\theta,t), \\ \dfrac{dV(\theta,t)}{d\theta} = -ku_r(\theta,t) + N(\theta,t) - \rho_l \dfrac{d^2u_r(\theta,t)}{dt^2}, \\ \dfrac{dM(\theta,t)}{Rd\theta} = V(\theta,t). \end{cases} \tag{17}$$

The uncoupled dynamic equation for the transverse displacement can be expressed as follows:

$$\frac{d^5u_r}{d\theta^5} + 2\frac{d^3u_r}{d\theta^3} + (1+\lambda^2)\frac{du_r}{d\theta} + \frac{\rho_l R^3}{EI}\frac{d^3u_r}{dt^2 d\theta} = 0. \tag{18}$$

These equations are subjected to the following boundary conditions:

$$\begin{cases} \left.\dfrac{du_{\theta 0}}{d\theta}\right|_{\theta=\varphi_C} = \left.\dfrac{du_{\theta 0}}{d\theta}\right|_{\theta=\pi} = 0, \\ u_r(\theta,0) = \dfrac{du_r(\theta,0)}{dt} = 0, \\ V(\varphi_C,t) = 0, \quad V(0,t) = -\dfrac{q'_r}{2}x(t), \\ \displaystyle\int_0^{\pi} u_{\theta 0}(\theta,t)d\theta = 0. \end{cases} \tag{19}$$

With the Laplace transformation and boundary conditions, using the transformation $L[u_r(t,\theta), t \to \zeta] = L(\zeta,\theta)$, where ζ is transform domain parameters, introducing the variable:

$$\Gamma_1 = \frac{1}{\lambda^2} = \frac{EI}{kR^3}, \quad \Gamma_2 = \frac{k}{R\rho_l}, \quad \Gamma_3 = \frac{kR}{q'_r},$$

$$\alpha' = \sqrt{\frac{\left(\sqrt{1+\dfrac{1}{\Gamma_1}+\dfrac{\zeta^2}{\Gamma_1\Gamma_2}}-1\right)}{2}}, \quad \beta' = \sqrt{\frac{\left(\sqrt{1+\dfrac{1}{\Gamma_1}+\dfrac{\zeta^2}{\Gamma_1\Gamma_2}}+1\right)}{2}},$$

where the following solution is given by:

$$\begin{aligned} L(\zeta,\theta) = \frac{R}{8\Gamma_1\Gamma_3\alpha'\beta'\zeta(\alpha'^2+\beta'^2)}\Bigg[& -\frac{4\alpha'\beta'}{(\alpha'^2+\beta'^2)\pi} \\ & + \frac{(\alpha' i+\beta')(e^{(\alpha'+i\beta')(\theta-\pi)} + e^{(\alpha'+i\beta')(\pi-\theta)})}{e^{(\alpha'+i\beta')\pi} - e^{-(\alpha'+i\beta')\pi}} \\ & - \frac{(\alpha' i-\beta')\left(e^{(\alpha'-i\beta')(\theta-\pi)} + e^{(\alpha'-i\beta')(\pi-\theta)}\right)}{e^{(\alpha'-i\beta')\pi} - e^{-(\alpha'-i\beta')\pi}}\Bigg]. \end{aligned} \tag{20}$$

Eqs. (20) is expected to be the radial displacement of elastic wheel changing with the harmonic impact load, the radial displacement ($\theta = 0$) is equal to the dynamic vertical deformation of MEW, the ratio of the deformation of elastic wheel with the vertical load is considered to be the dynamic stiffness of MEW.

4. Finite element modeling of mechanical elastic wheel and results analysis

4.1. Numerical model of elastic wheel material

The elastic wheel is mainly consisted of rubber material, cord ply and elastic bead ring as shown in Fig. 4. The distribution of the structure component material of elastic wheel determines the different stiffness characteristics of the MEW.

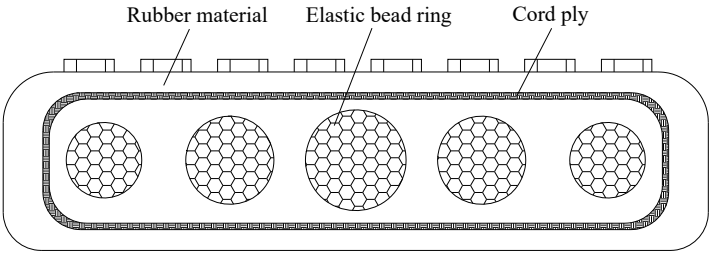

Fig. 4. Laminated structure of elastic wheel

The layers of tread and internal elastic wheel which consist of rubber material and composite material of cord are shown as laminated structure. Generally, rubber material is thought to be an isotropic hyper-elastic material, and its mechanical behavior can be described in terms of a proper strain energy density function. This kind of function has been used in the Rivlin and Ogden models. The Mooney-Rivlin model is commonly used as simplified forms of the Rivlin model. Introducing the variable $W = W(I_1, I_2, I_3)$ and $I_3 = 1$, the strain energy function W can be expressed as the Rivlin form:

$$W = \sum_{i=0,j=0}^{n} C_{ij}(I_1 - 3)^i (I_2 - 3)^j, \tag{21}$$

where I_1, I_2 and I_3 are respectively the first, second and third invariants, C_{ij} is the material constant:

$$I_1 = trE = E_{ii} = \lambda_1^2 + \lambda_2^2 + \lambda_3^2, \tag{22}$$

$$I_2 = \frac{1}{2}[(trE)^2 - trE^2] = E_{ii} = (\lambda_1\lambda_2)^2 + (\lambda_2\lambda_3)^2 + (\lambda_3\lambda_1)^2, \tag{23}$$

where λ_1, λ_2 and λ_3 are respectively the stretch ratios in three stretch directions, $\lambda_1\lambda_2\lambda_3 = 1$, $\partial W/\partial I_2$ far less than $\partial W/\partial I_1$, and the approximation is zero. Yeoh set up the strain energy intensity function in the form of $(I_1 - 3)$:

$$W = C_{10}(I_1 - 3) + C_{20}(I_1 - 3)^2 + C_{30}(I_1 - 3)^3. \tag{24}$$

Eq. (24) can be seen as the simplified form of the Rivlin model cubic equation, Yeoh pointed out that the Eq. (24) can fully describe the elastic mechanical performance of carbon black reinforcing rubber. This formula is suitable for tire rubber material, and material parameters can only be determined by the test of uniaxial tensile. Rubber material of elastic wheel is studied through uniaxial tensile test, using universal tensile tester from Instron Corporation. The

composite materials which consist with rubber and cord on wheel surface and inner layer are selected for the sample, unidirectional test is conducted for the composite materials under the condition of normal temperature. The test results of uniaxial tensile between stress and strain would be fitting, it obtains the material parameters of the Yeoh model, as shown in Table 1. The skeleton material parameters of MEW are given in Table 2.

Table 1. Material parameters of the Yeoh model

Components	C_{10} (MPa)	C_{01} (MPa)	C_{20} (MPa)	C_{30} (MPa)	ρ (kg/m^3)
Rubber tread	0.563672	0.004359			1.279×10^3
Rubber inner lay	0.467153	0.003276			1.256×10^3
Cord ply	0.706438		4.92317	4.13675	1.217×10^3

Table 2. The properties of MEW

Components	Young's modulus (MPa)	Poisson's ratio	Density (kg/m^3)
Elastic bead ring	1.96×10^5	0.30	7.81×10^3
Hinges	2.10×10^5	0.29	7.85×10^3
Hub	2.10×10^5	0.30	7.80×10^3

The above analysis shows that the component content of cord and rubber changes with the percentage of elastic bead ring, under this circumstance that the cross-section of the elastic wheel has been unchanged. According to the sensitivity analysis, the effect of the component content of cord and rubber on equivalent stiffness of elastic wheel is relatively small. Thus, the maximum influence of the component content of the elastic bead ring on equivalent modulus is studied.

4.2. Finite element model of MEW

To appropriately simplify the MEW model, the three-dimensional geometric model of elastic wheel, hinges and hub are established using the software Pro/E, without considering the tread patterns. The hinges can be simplified into 12 groups of three bar linkage and the hub ignores the irregular interface shape which almost has no influence to solution precision. The CAD model of MEW is imported into ABAQUS, and the 3D finite element model adopts C3D10M elements. The FEM contains 52164 elements and 150572 nodes. The elastic bead ring is also modeled by solid elements. The cord ply comprises cord-rubber composite which displays the mechanics anisotropy and non-linearity, and it is modeled using the rebar layer. The stiffness calculations for the rebar elements use the same integration nodes as the calculation for the underlying rubber shell elements. The FEM of the MEW is shown in Fig. 5.

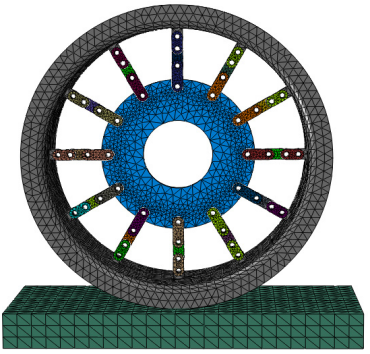

Fig. 5. FEM model of the MEW

4.3. Loading and boundary conditions

The contact between the MEW and the ground is a contact of large displacement and

non-linearity, separating into static state and dynamic state. In order to prevent the possible contact between nodes penetrate, the ground is simulated using the rigid wall. The rigid ground is fixed, the MEW produces radial deformation under the function of load, and the distribution of deformation displacement of MEW under the certain load is shown in Fig. 6. In the process of the non-rolling dynamic stiffness simulation of MEW, the wheel is vibrated by the different frequencies of harmonic impact load in the certain pre loading conditions.

The upper part of elastic wheel appears elliptic elastic deformation under the action of the downward tension of suspended hub. The distance from the bottom of elastic wheel to the hub is less than the length of the hinges due to the vertical displacement of hub. According to the design of wheel structure, the hinges only load on tension rather than pressure, and the hinges that located at the bottom of elastic wheel appear the different bending deformation. Under the action of vertical load, the hinges that closer to the ground are curved, and the hinges that located at either side of the contact point between the MEW and the ground also appear micro bending deformation, the state is shown in the magnified area of Fig. 6.

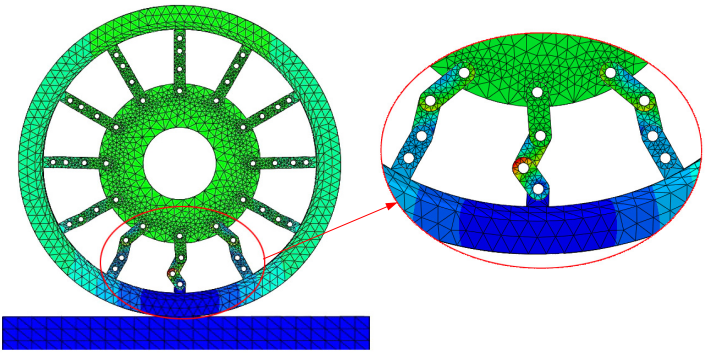

Fig. 6. Distribution of deformation displacement of MEW under the certain load

4.4. Parametric analysis and model validation

The motion of MEW can be seen as the hub driving elastic wheel rotation through the hinges. According to the rotation of elastic wheel lags behind the hub, a lag angle between the hinges and the hub is generated in the process of the motion of MEW. Compared with the static deformation, the compression deformation of the hinges can be relieved under the certain rotation speed, the state is shown in Fig. 7. With the increase of the rotation speed of MEW, the lag angle between the hinges and the hub is gradually increased. The compression of the hinges is gradually elongated. The lag angle and the state of distribution hinges are no longer changed when the rotation speed of MEW is 5.91 rad/s, and it makes the MEW rotation in the condition that the equilibrium state of internal structure remains unchanged.

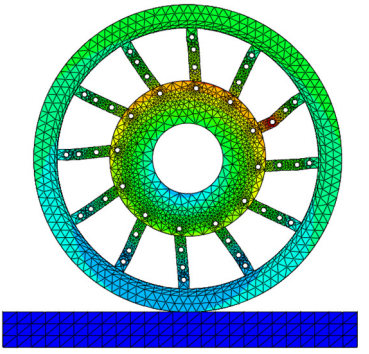

Fig. 7. Deformation of the MEW under the certain rotation speed

Under the certain load, the radial displacement and contact pressure distribution of elastic wheel are obtained using the curved beam and nonlinear finite element model, as shown in Fig. 8. The relation between the total load and deflection is obtained by the analytical solution and finite element approaches as shown in Fig. 9.

The analytical solution and finite element method results are in excellent agreement for the displacement and contact pressure distribution in Fig. 8 and Fig. 9. The correctness of the curved beam model has been validated, and it indicates that the model of wheel on the basis of curved beam will be used as a theoretical basis to study the mechanical characteristics. The reason for deviation is mainly that the porosity of elastic bead ring is ignored in the simplified model, resulting in the static stiffness value of analytical model is slightly larger. The data analysis indicates that, the equivalent stiffness of wheel has become increased with the deformation of wheel, it displays that the characteristics to some extent are nonlinear, in the condition that the component contents of the laminated structure of elastic wheel are certain.

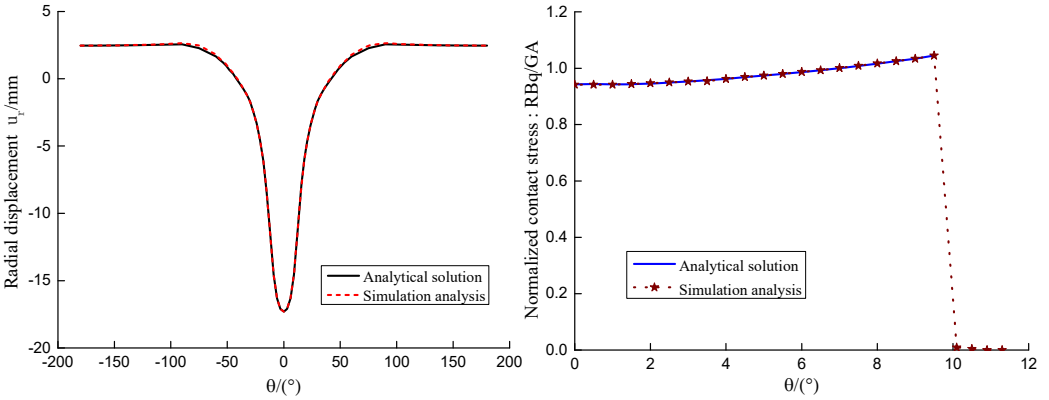

Fig. 8. Comparison of radial displacement and contact pressure obtained analytically and from the finite element method

5. Influencing factors analysis

The equivalent stiffness consists of radial stiffness of elastic wheel and elastic foundation stiffness of hinges, it is as known as static stiffness of the MEW. It mainly depends on the component content of laminated structure of elastic wheel and the circumferential distribution of the number of hinges. The influence of changing the laminated structure of elastic wheel on circumferential stiffness, bending stiffness and shear stiffness, and the static stiffness of wheel has become increased with equivalent modulus. The response of MEW is considered to be the dynamic response under a harmonic force, and it is as known as the change regularity of dynamic stiffness. According to the preliminary determined of the topological structure of MEW, the influence of changing component content of elastic bead ring in the laminated structure of elastic wheel on static stiffness and dynamic response are analyzed by the curved beam and finite element model, under this circumstance that the number of hinges has been unchanged.

5.1. Influence of the laminated structure of elastic wheel on equivalent stiffness

The equivalent and shear modulus of elastic wheel has become increased with component content of elastic bead ring, under this circumstance that the cross-section of elastic wheel has been unchanged. The equivalent stiffness of MEW is perturbed in a certain range, the influence law as shown in Fig. 10.

Fig. 10 illustrates the influence of changing component content of elastic bead ring on equivalent stiffness, the equivalent stiffness of wheel has become increased nonlinearly with

component content of elastic bead ring. The equivalent stiffness of MEW increases rapidly, when the contents of elastic bead ring are less than 8.83 %, and the added value of equivalent stiffness accounts for 29.84 % of the initial design value, while the contents of elastic bead ring has increased from 8.27 % to 13.74 %. The application of the nonlinear finite element model shows that the elastic wheel will appear local convex under the maximum allowable load, when the contents of elastic bead ring are less than 6.73 %. The grip performance of MEW decreased significantly while the contents of elastic bead ring are more than 13.74 %.

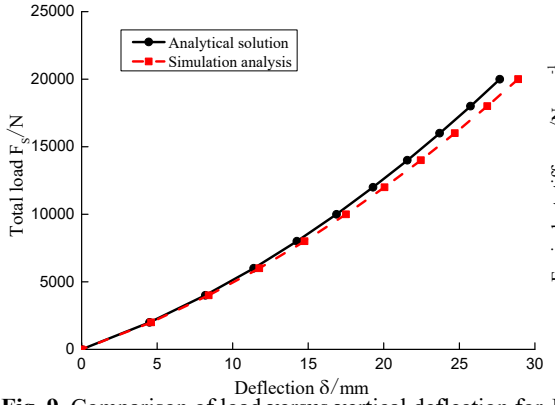

Fig. 9. Comparison of load versus vertical deflection for the analytical and finite element approaches

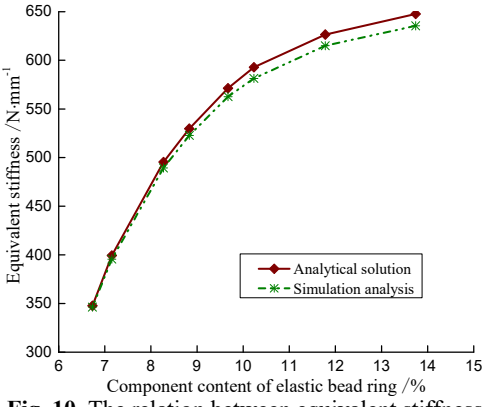

Fig. 10. The relation between equivalent stiffness and component content of elastic bead ring

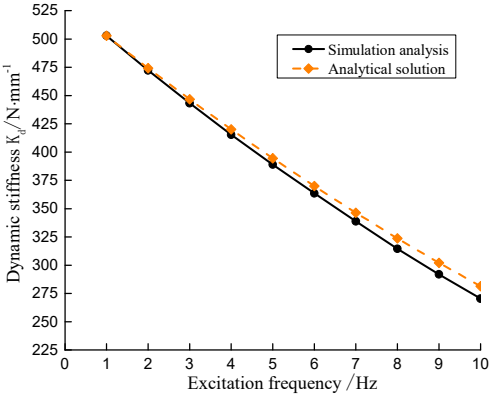

Fig. 11. The relation between dynamic stiffness and excitation frequency

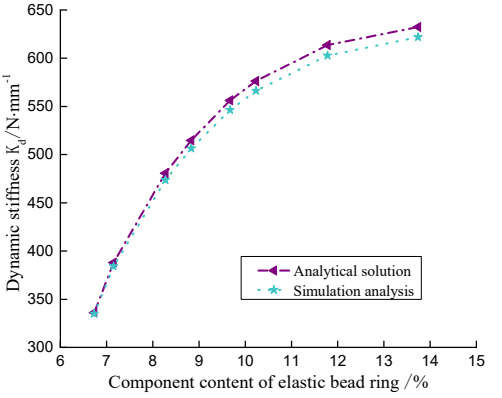

Fig. 12. The relation between dynamic stiffness and component content of elastic bead ring

5.2. Influence of the laminated structure of elastic wheel on dynamic response

The component content of laminated structure of elastic wheel, deformation amount of the wheel and excitation frequency has greater influence on the dynamic response of MEW. The influence of excitation frequency on the dynamic stiffness of MEW is shown in Fig. 11, under this circumstance that the laminated structure of elastic wheel has been unchanged. The influence of component contents of elastic bead ring on the dynamic stiffness of MEW is shown in Fig. 12, in the condition that the excitation frequency has been unchanged.

Fig. 11 and Fig. 12 illustrate the dynamic stiffness of wheel have become increased significantly with excitation frequency. The influence of the elastic wheel laminated structure and deformation on dynamic response is equal to the equivalent stiffness under a certain excitation frequency. The application of the nonlinear finite element model shows that the buffering performance of MEW decreased significantly while the contents of elastic bead ring are more than 13.74 %.

The research ideas of this paper and solution of the problem were proposed by Qiang Wang. Professor Youqun Zhao contributed to the guarantor of integrity of entire study, and gave a guide to the solution of the research problem and the writing style. Xianbin Du provided some help in the process of finite element modeling. Mingmin Zhu provided some help in the writing style. Hongxun Fu helped perform the Partial data processing.

6. Conclusion

1) The elastic foundation closed circle curved beam model is established based on the curved beam theory. Meanwhile, the stress distributions of contact region and non-contact region of the elastic wheel are analyzed respectively, and the influences of bending stiffness of elastic wheel, elastic foundation stiffness of hinges and excitation frequency on the equivalent stiffness and dynamic stiffness are also obtained.

2) The analytical solution of curved beam model and finite element method results are in excellent agreement for the displacement and contact pressure distribution. The correctness of the curved beam model has been validated, and it indicates that the model of wheel on the basis of curved beam will be used as a theoretical basis to study the mechanical characteristics. The equivalent and dynamic stiffness of MEW increase nonlinearly with the deformation amount of the wheel, in the condition that the laminated structure of elastic wheel has been unchanged.

3) The equivalent stiffness of wheel has become increased nonlinearly with component content of elastic bead ring. The equivalent stiffness of MEW increases rapidly, when the contents of elastic bead ring are less than 8.83 %, the added value of equivalent stiffness accounts for 29.84 % of the initial design value, while contents of elastic bead ring has increased from 8.27 % to 13.74 %. The influence of the laminated structure and deformation of elastic wheel on dynamic response is equal to the equivalent stiffness under a certain excitation frequency. The dynamic response significantly decreases with the increase of excitation frequency, under this circumstance that the laminated structure of elastic wheel has been unchanged.

Acknowledgements

The authors give sincere thanks to the editors and the reviewers for their patient work and constructive suggestions. This research work is supported by the Major Exploration Project of the General Armaments Department of China (No. NHA13002), the Fundamental Research Funds for the Central Universities (No. 56XBC16012), and Funding of Jiangsu Innovation Program for Graduate Education and the Fundamental Research Funds for the Central Universities (No. KYLX_0241).

References

[1] **Tonkovich Aleksander, Li Zhanbiao, DiCecco Sante, et al.** Experimental observations of tyre deformation characteristics on heavy mining vehicles under static and quasi-static loading. Journal of Terramechanics, Vol. 49, Issues 3-4, 2012, p. 215-231.

[2] **Guan Yanjin, Cheng Gang, Zhao Guoqun, et al.** Investigation of the vibration characteristics of radial tires using experimental and numerical techniques. Journal of Reinforced Plastics and Composites, Vol. 30, Issue 24, 2011, p. 2035-2050.

[3] **Ramji K., Goel V. K., Saran V. H.** Stiffness properties of small-sized pneumatic tyres. Journal of Automobile Engineering, Vol. 216, Issue 2, 2002, p. 107-114.

[4] **Wang Wei, Yan Shan, Zhao Shugao** Experimental verification and finite element modeling of radial truck tire under static loading. Journal of Reinforced Plastics and Composites, Vol. 32, Issue 7, 2013, p. 490-498.

[5] **Winroth J., Andersson P. B. U., Kropp W.** Importance of tread inertia and damping on the tyre/road contact stiffness. Journal of Sound and Vibration, Vol. 333, Issue 21, 2014, p. 5378-5385.

[6] **Gruber P., Sharp Crocombe R. S. A. D.** Friction and camber influences on the static stiffness properties of a racing tyre. Journal of Automobile Engineering, Vol. 222, Issue 11, 2008, p. 1965-1976.

[7] **Miège A. J. P., Popov A. A.** Truck tyre modelling for rolling resistance calculations under a dynamic vertical load. Journal of Automobile Engineering, Vol. 219, Issue 4, 2005, p. 441-456.

[8] **Carman K.** Prediction of soil compaction under pneumatic tires using fuzzy logic approach. Journal of Terramechanics, Vol. 45, Issue 4, 2008, p. 103-108.

[9] **Kim Byoung Sam, Chi Chang Heon, Lee Tae Keun** A study on radial directional natural frequency and damping ratio in a vehicle tire. Applied Acoustics, Vol. 68, Issue 5, 2007, p. 538-556.

[10] **Wang Wei, Zhao Youqun, Wang Jian, et al.** Structure analysis and ride comfort of vehicle on new mechanical elastic tire. Proceedings of the FISITA 2012 World Automotive Congress, Springer-Verlag, Heidelberg, Berlin, Vol. 10, 2013, p. 199-209.

[11] **Wang Wei, Zhao Youqun, Huang Chao, et al.** Modeling and trafficability analysis of new mechanical elastic wheel. China Mechanical Engineering, Vol. 24, Issue 6, 2013, p. 724-729, (in Chinese).

[12] **Zang Liguo, Zhao Youqun, Li Bo, et al.** Influence of mechanical elastic wheel configuration for traction ability. Journal of Harbin Engineering University, Vol. 35, Issue 11, 2014, p. 1-6, (in Chinese).

[13] **Kim Kwangwon, Kim Seunghye, Kim Doo-Man, et al.** Contact pressure of non-pneumatic tires with hexagonal lattice spokes. Proceedings of the ASME 2011 International Mechanical Engineering Congress and Exposition, Denver, USA, 2011.

[14] **Lee Chihun, Ju Jaehyung, Kim Doo-Man** The dynamic properties of a non-pneumatic tire with flexible auxetic honeycomb spokes. Proceedings of the ASME 2012 International Mechanical Engineering Congress and Exposition, Houston, USA, 2012.

[15] **Ju Jaehyung, Kim Doo-Man, Kim Kwangwon** Flexible cellular solid spokes of a non-pneumatic tire. Composite Structures, Vol. 94, Issue 8, 2012, p. 2285-2295.

[16] **Gasmi Amir, Joseph Paul F., Rhyne Timothy B., et al.** Closed-form solution of a shear deformable, extensional ring in contact between two rigid surfaces. International Journal of Solids and Structures, Vol. 48, Issue 5, 2011, p. 843-853.

[17] **Gasmi Amir, Joseph Paul F., Rhyne Timothy B., et al.** Development of a two-dimensional model of a compliant non-pneumatic tire. International Journal of Solids and Structures, Vol. 49, Issue 13, 2012, p. 1723-1740.

[18] **Lin K. C., Hsieh C. M.** The closed form general solutions of 2-D curved laminated beams of variable curvatures. Composite Structures, Vol. 79, Issue 4, 2007, p. 606-618.

[19] **Ju J., Ananthasayanam B., Summers J. D., et al.** Design of cellular shear bands of a non-pneumatic tire-investigation of contact pressure. SAE International Journal of Passenger Cars-Mechanical Systems, Vol. 3, Issue 1, 2010, p. 598-606.

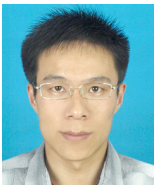

Qiang Wang received the M.S. degree in Mechanical and Power Engineering Institute from Nanjing TECH University, Nanjing, China, in 2011. Now he is a Ph.D. student in School of Energy and Power Engineering, NUAA. His current research interests include tire dynamic, vibration analysis, vehicle dynamic simulation and control.

Youqun Zhao received the B.S., M.S. and Ph.D. degrees from Jilin University, Changchun, China, in 1990, 1993 and 1998, respectively. Now he is a professor in Vehicle Engineering of NUAA. His current research interests include tire dynamic, vibration analysis, vehicle dynamic simulation and control.

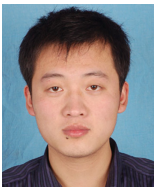

Xianbin Du received the M.S. degree in Shandong University of Technology, Zibo, China, in 2013. Now he is a Ph.D. student in School of Energy and Power Engineering, NUAA. His current research interests include tire dynamic and vehicle dynamic simulation and control.

Mingmin Zhu received the M.S. degree in Jiangsu University of Science and Technology, Zhenjiang, China, in 2015. Now he is a Ph.D. student in School of Energy and Power Engineering, NUAA. His current research interests include tire dynamic and vibration analysis

Hongxun Fu received the M.S. degree in Shandong University of Technology, Zibo, China, in 2012. Now he is a Ph.D. student in School of Energy and Power Engineering, NUAA. His current research interests include tire dynamic and vehicle dynamic simulation and control.